

Core mass – halo mass relation of bosonic and fermionic dark matter halos harbouring a supermassive black hole

Pierre-Henri Chavanis*

Laboratoire de Physique Théorique, Université de Toulouse, CNRS, UPS, France

We study the core mass – halo mass relation of bosonic dark matter halos, in the form of self-gravitating Bose-Einstein condensates, harbouring a supermassive black hole. We use the “velocity dispersion tracing” relation according to which the velocity dispersion in the core $v_c^2 \sim GM_c/R_c$ is of the same order as the velocity dispersion in the halo $v_h^2 \sim GM_h/r_h$ (this relation can be justified from thermodynamical arguments) and the approximate analytical mass-radius relation of the quantum core in the presence of a central black hole obtained in our previous paper [P.H. Chavanis, *Eur. Phys. J. Plus* **134**, 352 (2019)]. For a given minimum halo mass $(M_h)_{\min} \sim 10^8 M_\odot$ determined by the observations, the only free parameter of our model is the scattering length a_s of the bosons (their mass m is then determined by the characteristics of the minimum halo). For noninteracting bosons and for bosons with a repulsive self-interaction, we find that the core mass M_c increases with the halo mass M_h and achieves a maximum value $(M_c)_{\max}$ at some halo mass $(M_h)_*$ before decreasing. The whole series of equilibria is stable. For bosons with an attractive self-interaction, we find that the core mass achieves a maximum value $(M_c)_{\max}$ at some halo mass $(M_h)_*$ before decreasing. The series of equilibria becomes unstable above a maximum halo mass $(M_h)_{\max} \geq (M_h)_*$. In the absence of black hole $(M_h)_{\max} = (M_h)_*$. At that point, the quantum core (similar to a dilute axion star) collapses. We perform a similar study for fermionic dark matter halos. We find that they behave similarly to bosonic dark matter halos with a repulsive self-interaction, the Pauli principle for fermions playing the role of the repulsive self-interaction for bosons.

PACS numbers: 95.30.Sf, 95.35.+d, 98.62.Gq

I. INTRODUCTION

The nature of dark matter (DM) is still unknown and remains one of the greatest mysteries of modern cosmology. The standard cold dark matter (CDM) model, assuming the existence (still hypothetical) of weakly interacting massive particles (WIMPs) of mass $m \sim \text{GeV}/c^2$, works remarkably well at large (cosmological) scales [1, 2] but encounters serious problems at small (galactic) scales that are referred to as the “cusp-core problem” [3, 4], the “missing satellite problem” [5], and the “too big to fail problem” [6]. The expression “small-scale crisis of CDM” has been coined. In order to solve these problems, some authors have proposed to take the quantum nature of the DM particle into account (see an exhaustive list of references in Refs. [7, 8] and in the reviews [9–14]). Indeed, quantum mechanics creates an effective pressure even at zero thermodynamic temperature ($T_{\text{th}} = 0$) that may balance the gravitational attraction at small scales and lead to cores instead of cusps. The DM particle could be a fermion, like a massive neutrino, or a boson in the form of a Bose-Einstein condensate (BEC), like an ultralight axion. In order to match the characteristics of the smallest halos like dwarf spheroidals (dSphs) that are interpreted as purely quantum objects (see below), the mass of the fermion should be of the order of $m \sim 170 \text{ eV}/c^2$ while the mass of the boson should be of the order of $m \sim 2.92 \times 10^{-22} \text{ eV}/c^2$ if it has a vanishing

self-interaction, or lie in the range $2.19 \times 10^{-22} \text{ eV}/c^2 < m < 2.92 \times 10^{-22} \text{ eV}/c^2$ if it has an attractive self-interaction, and in the range $2.92 \times 10^{-22} \text{ eV}/c^2 < m < 1.10 \times 10^{-3} \text{ eV}/c^2$ if it has a repulsive self-interaction (see Appendix D of [15] and Ref. [16]).¹

In these quantum models, sufficiently large DM halos have a “core-halo” structure which results from a process of violent collisionless relaxation [20] and gravitational cooling [21–23]. This core-halo structure has been evidenced in direct numerical simulations of noninteracting BECDM [24–28]. The quantum core stems from the equilibrium between the quantum pressure and the gravitational attraction (ground state).² Quantum mechanics

¹ These values are indicative. They are orders of magnitude that could be improved by making a more detailed comparison with observations. The arguments of [15, 16] suggest that the mass of a boson with an attractive self-interaction should be slightly smaller than the mass of a noninteracting boson ($m \sim 2.92 \times 10^{-22} \text{ eV}/c^2$), while the mass of a boson with a repulsive self-interaction can be up to 20 orders of magnitude larger than the mass of a noninteracting boson. As discussed in Appendix D.4 of [15], a mass larger than $2.92 \times 10^{-22} \text{ eV}/c^2$ could alleviate some tensions with the observations of the Lyman- α forest encountered in the noninteracting model. As a result, a repulsive self-interaction ($a_s > 0$) is privileged over an attractive self-interaction ($a_s < 0$). A repulsive self-interaction is also favored by cosmological constraints [15, 17]. In this respect, we recall that theoretical models of particle physics usually lead to particles with an attractive self-interaction (e.g., the QCD axion). However, some authors [18, 19] have pointed out the possible existence of particles with a repulsive self-interaction (e.g., the light majoron).

² The quantum pressure arises from the Pauli exclusion principle

*Electronic address: chavanis@irsamc.ups-tlse.fr

stabilizes DM halos against gravitational collapse, leading to flat cores instead of cusps. The core mass-radius relation $M_c(R_c)$ can be obtained numerically by solving the differential equation of quantum hydrostatic equilibrium [29], or approximately by making a Gaussian ansatz for the density profile [7]. On the other hand, the halo (atmosphere) is relatively independent of quantum effects. It is similar to the Navarro-Frenk-White (NFW) profile [3] produced in CDM simulations or to the empirical Burkert profile [4] deduced from the observations.³ It is responsible for the flat rotation curves of the galaxies at large distances. We shall approximate this halo by an isothermal sphere with an effective temperature T as in the theory of violent relaxation based on the Vlasov equation [20] (see [32] for the Schrödinger-Vlasov correspondence). In that case, the density decreases at large distances as $\rho \propto r^{-2}$ [33], instead of r^{-3} for the NFW and Burkert profiles, leading exactly to flat rotation curves for $r \rightarrow +\infty$. For sufficiently large DM halos, the halo mass-radius relation is given by [8]

$$M_h = 1.76 \Sigma_0 r_h^2, \quad (1)$$

where

$$\Sigma_0 = \rho_0 r_h = 141 M_\odot / \text{pc}^2 \quad (2)$$

is the universal surface density of DM halos deduced from the observations [34–36]. Ultracompact halos like dSphs ($r_h \sim 1 \text{ kpc}$ and $M_h \sim 10^8 M_\odot$) are dominated by the quantum core and have almost no atmosphere. They correspond to the ground state of the quantum model. Large halos like the Medium Spiral ($r_h \sim 10 \text{ kpc}$ and $M_h \sim 10^{11} M_\odot$) are dominated by the isothermal atmosphere.

A fundamental problem in the physics of quantum DM halos is to determine the relation $M_c(M_v)$ between the quantum core mass M_c and the halo mass M_v . In the case of noninteracting bosons, the scaling $M_c \propto M_v^{1/3}$ was obtained numerically by Schive *et al.* [25] (see also [27]) and explained with a heuristic argument based on a wavelike “uncertainty principle”. It was then observed by several authors [8, 26, 37] that this relation could be obtained from a “velocity dispersion tracing” relation according to which the velocity dispersion in the core $v_c^2 \sim GM_c/R_c$

is of the same order as the velocity dispersion in the halo $v_v^2 \sim GM_v/r_v$. In recent papers [8, 16], we managed to justify this relation from an effective thermodynamic approach. We considered DM halos with a quantum core and an homogeneous isothermal atmosphere in a box of radius r_h . We analytically computed the free energy $F(M_c)$ and the entropy $S(M_c)$ of this core-halo configuration as a function of the core mass M_c . The equilibrium core mass was then determined by extremizing the free energy $F(M_c)$ at fixed halo mass M_h , or by extremizing the entropy $S(M_c)$ at fixed halo mass M_h and energy E_h (these extremization problems are equivalent). In this manner, we could obtain the core mass M_c as a function of the halo mass M_h . We showed that the resulting relation is equivalent to the “velocity dispersion tracing” relation $GM_c/R_c \sim GM_v/r_v$. We could therefore provide a justification of the “velocity dispersion tracing” relation from thermodynamical arguments. We also showed that the core-halo configuration is a maximum of free energy (instead of being a minimum) so that it is unstable in the canonical ensemble. In particular, it has a negative specific heat which is forbidden in the canonical ensemble. However, the statistical ensembles are inequivalent for systems with long-range interactions like gravitational systems [38–40]. We could then show that, if the halo mass is not too large, the core-halo configuration is a maximum of entropy at fixed mass and energy so that it is stable in the microcanonical ensemble. This makes the core-halo configuration extremely important since it corresponds to the “most probable” configuration of the system (in a thermodynamical sense). Finally, using the “velocity dispersion tracing” relation, we could generalize the core mass – halo mass relation obtained by Schive *et al.* [25] to the case of DM halos made of bosons with attractive or repulsive interaction and to the case of DM halos made of fermions [8, 16].

Based on these results, we have developed the following scenario which is valid for bosons and fermions (see Fig. 49 of [8] for an illustration of this scenario in the case of bosons with a repulsive self-interaction). There exists a “minimum halo” of mass $(M_h)_{\min}$ corresponding to the ground state of the quantum gas ($T = 0$) at which the DM halo is a purely quantum object without isothermal atmosphere ($M_c \simeq M_h$). Observations reveal that $(M_h)_{\min} \sim 10^8 M_\odot$. Above a canonical critical point $(M_h)_{\text{CCP}}$, the DM halos have a core-halo structure with a quantum core and an isothermal atmosphere. The quantum core may mimic a galactic nucleus or a large bulge, but it cannot mimic a central black hole (BH). At the beginning of this branch, the core-halo structure is stable in the microcanonical ensemble and the core mass M_c increases with the halo mass M_h .⁴ Above a microcanonical

for fermions and from the Heisenberg uncertainty principle for bosons. A repulsive self-interaction may also help stabilizing the quantum core. By contrast, an attractive self-interaction tends to destabilize the quantum core above a maximum mass $M_{\max} = 1.012 \hbar / \sqrt{Gm|a_s|}$ identified in [7].

³ In the case of BECDM, the halo is due to quantum interferences of excited states. It is made of granules (quasiparticles) of the size of the solitonic core $\lambda_{\text{dB}} \sim \hbar/mv \sim 1 \text{ kpc}$ (de Broglie wavelength) and of effective mass $m_* \sim \rho \lambda_{\text{dB}}^3 \sim 10^7 M_\odot \gg m$ [24, 25, 30, 31]. These supermassive granules can cause the “collisional” relaxation of the halo on a timescale smaller than the age of the universe (by contrast, the relaxation due to the ultralight particles of mass m would be completely negligible).

⁴ We also found a branch along which the core mass M_c decreases as the halo mass M_h increases. Rapidly, the core mass becomes negligible and the halos behave as purely isothermal halos with-

critical point $(M_h)_{\text{MCP}}$, the core-halo structure becomes thermodynamically unstable and the quantum core is replaced by a supermassive black hole (SMBH) resulting from a gravothermal catastrophe [41] followed by a dynamical instability of general relativistic origin [42]. In that process the halo is left undisturbed and conserves its approximately isothermal structure. The gravothermal catastrophe is a slow (secular) process but it may be relevant in galactic nuclei or if the DM particle has a self-interaction [42]. In conclusion, we predicted in [8, 16] that DM halos with a mass $(M_h)_{\text{min}} < M_h < (M_h)_{\text{CCP}}$ are purely quantum objects while DM halos with a mass $M_h > (M_h)_{\text{CCP}}$ have a core-halo structure with an approximately isothermal atmosphere. In the latter case, DM halos with a mass $(M_h)_{\text{CCP}} < M_h < (M_h)_{\text{MCP}}$ harbour a quantum core (bosonic soliton or fermion ball) while DM halos with a mass $M_h > (M_h)_{\text{MCP}}$ harbour a SMBH. These results are connected to the fundamental existence of a canonical and a microcanonical critical point in the statistical mechanics of self-gravitating systems [40].

The previous scenario, if correct, could explain the formation of SMBHs at the centers of DM halos resulting from the collapse of the quantum core above a maximum halo mass $(M_h)_{\text{MCP}}$. However, it is also possible that DM halos of any size harbour a SMBH that was present prior to the formation of the quantum core. Actually, it is observed that most galaxies harbour a SMBH and that the SMBH mass M_{BH} is correlated with the velocity dispersion σ of the hot-galaxy bulge, leading to the so-called $M_{\text{BH}} - \sigma$ relation. As a result, the SMBH mass is also correlated with global halo properties such as the total halo mass M_v , leading to the BH mass – halo mass relation $M_{\text{BH}}(M_v)$. In that case, we must revise our scenario [8, 16] by taking into account the influence of the BH on the mass-radius relation of the quantum core. To simplify the problem, we shall treat the BH as a point mass. In that case, the mass-radius relation $M_c(R_c)$ of the quantum core has been obtained in [43] by using approximate analytical methods based on a Gaussian ansatz for the density profile. We shall also use the “velocity dispersion tracing” relation $GM_c/R_c \sim GM_h/r_h$, assuming that this relation remains valid in the presence of a SMBH. From the BH mass – halo mass relation $M_{\text{BH}}(M_h)$, the core mass-radius relation $M_c(R_c)$, the “velocity dispersion tracing” relation $GM_c/R_c \sim GM_h/r_h$ and the halo mass-radius relation $M_h = 1.76 \Sigma_0 r_h^2$, we can obtain the core mass – halo mass relation $M_c(M_h)$. This is the subject of the present paper.⁵ After recalling general results

in Sec. II, we treat the case of bosonic DM halos in Sec. III and the case of fermionic DM halos in Sec. IV.

II. GENERAL RESULTS

A. The BH mass – halo mass relation

Most galaxies are known to harbour a SMBH of millions of solar masses at their center. It is found from observations that the BH mass – halo mass relation is given by [50, 51]

$$\frac{M_{\text{BH}}}{M_\odot} = 1.07 \times 10^{-12} \left(\frac{M_v}{M_\odot} \right)^{1.55}, \quad (3)$$

where M_v is the virial halo mass. In our previous papers [8, 16], we have worked with the halo mass M_h defined such that M_h is the mass contained within the sphere of radius r_h where the central density has been divided by four (i.e. $\rho_h = \rho_0/4$). These two masses are related by [16]

$$\frac{M_h}{(M_h)_{\text{min}}} \sim B \left[\frac{M_v}{(M_h)_{\text{min}}} \right]^{4/3}, \quad (4)$$

where

$$B = \frac{1}{1.76 \Sigma_0} \left[\frac{4}{3} \pi \zeta(0) \rho_{m,0} \right]^{2/3} (M_h)_{\text{min}}^{1/3}. \quad (5)$$

In this expression, $\rho_{m,0} = 2.66 \times 10^{-24} \text{ g cm}^{-3}$ is the present background matter density in the Universe, $\zeta(0)$ is a prefactor of order 350, and $(M_h)_{\text{min}}$ is the minimum mass of the DM halos observed in the Universe. If we take $(M_h)_{\text{min}} = 10^8 M_\odot$, a choice that we will make subsequently, we obtain $B = 2.79 \times 10^{-3}$. Therefore

$$\frac{M_h}{(M_h)_{\text{min}}} \sim 2.79 \times 10^{-3} \left[\frac{M_v}{(M_h)_{\text{min}}} \right]^{4/3}. \quad (6)$$

Combining the foregoing relations, we get

$$\frac{M_{\text{BH}}}{(M_h)_{\text{min}}} = 2.69 \times 10^{-8} \left(\frac{M_v}{(M_h)_{\text{min}}} \right)^{1.55} \quad (7)$$

and

$$\frac{M_{\text{BH}}}{(M_h)_{\text{min}}} = 2.51 \times 10^{-5} \left(\frac{M_h}{(M_h)_{\text{min}}} \right)^{1.16}. \quad (8)$$

⁵ out quantum core.

⁵ While our paper was in preparation, we came across the interesting paper of Davies and Mocz [44] who consider fuzzy DM soliton cores (made of noninteracting bosons) around SMBHs. These authors assume that the $M_c(M_h)$ relation is unchanged by the presence of the SMBH. This is valid if the soliton forms early in the history of the Universe, before the SMBH. In our study,

we make the opposite assumption and study how the $M_c(M_h)$ relation is affected by the presence of the SMBH. A comparison between the two studies is made in Sec. V. The effects of a SMBH on BECDM halos have also been studied recently by Avilez *et al.* [45], Eby *et al.* [46], Bar *et al.* [47], Chavanis [43] and Brax *et al.* [48]. On the other hand, Desjacques and Nusser [49] consider the possibility that soliton cores on galactic nuclei may mimic SMBHs.

For the sake of generality, we write the BH mass – halo mass relation under the form

$$\frac{M_{\text{BH}}}{(M_h)_{\text{min}}} = A \left(\frac{M_h}{(M_h)_{\text{min}}} \right)^a, \quad (9)$$

where the constants A and a can be updated if necessary. From the results of [51], their values are $A = 2.51 \times 10^{-5}$ and $a = 1.16$.

B. Velocity dispersion tracing relation

To obtain the core mass – halo mass relation $M_c(M_h)$ we shall use the velocity dispersion tracing relation

$$v_c^2 \sim v_h^2 \quad \text{or} \quad M_c \sim \frac{R_c}{r_h} M_h, \quad (10)$$

stating that the velocity dispersion in the core $v_c^2 \sim GM_c/R_c$ is of the same order as the velocity dispersion in the halo $v_h^2 \sim GM_h/r_h$. This relation was introduced in [8, 26, 37]. It was shown to reproduce the core mass – halo mass relation obtained numerically by Schive *et al.* [25] for noninteracting bosons. In recent papers [8, 16], we have provided a justification of this relation from an effective thermodynamic approach by determining the core mass that maximizes the entropy of the DM halo at fixed total mass and energy. We showed that this relation remains valid for self-interacting bosons and for fermions. In the present paper, we assume that it also remains valid when the halo contains a central BH. Using the halo mass – radius relation $M_h = 1.76 \Sigma_0 r_h^2$ [see Eq. (1)],⁶ we can rewrite Eq. (10) as

$$\frac{M_c}{R_c} \sim \sqrt{1.76 \Sigma_0 M_h}. \quad (11)$$

III. BOSONIC DM HALOS

In this section, we obtain the core mass – halo mass relation of bosonic DM halos in the presence of a central BH by combining the velocity dispersion tracing relation (11) with the core mass-radius relation of a self-gravitating BEC at $T = 0$.

A. Core mass-radius relation

A self-gravitating BEC is basically described by the Gross-Pitaevskii-Poisson (GPP) equations (see, e.g., [7]). Far from the Schwarzschild radius, we can treat the central BH as a point mass creating an external potential

$\Phi_{\text{ext}} = -GM_{\text{BH}}/r$. Using a Gaussian ansatz for the wave function, we found in [43] that the approximate mass-radius relation of a self-gravitating BEC at $T = 0$ (ground state) with a central BH is given by

$$M_c = \frac{2\sigma}{\nu} \frac{\frac{\hbar^2}{Gm^2 R_c} - \frac{\lambda}{2\sigma} M_{\text{BH}}}{1 - \frac{6\pi\zeta a_s \hbar^2}{\nu Gm^3 R_c^2}} \quad (12)$$

with the coefficients $\sigma = 3/4$, $\zeta = 1/(2\pi)^{3/2}$, $\nu = 1/\sqrt{2\pi}$ and $\lambda = 2/\sqrt{\pi}$. Inversely, the radius of the BEC can be expressed in terms of its mass by

$$R_c = \frac{\sigma}{\nu} \frac{\hbar^2}{Gm^2} \frac{1}{M_c + \frac{\lambda}{\nu} M_{\text{BH}}} \times \left[1 \pm \sqrt{1 + \frac{6\pi\zeta\nu}{\sigma^2} \frac{Gma_s}{\hbar^2} M_c \left(M_c + \frac{\lambda}{\nu} M_{\text{BH}} \right)} \right] \quad (13)$$

with $+$ when $a_s > 0$ and with \pm when $a_s < 0$. When $M_{\text{BH}} = 0$, we recover the approximate mass-radius relation obtained in [7]. The results of [7, 43] apply to the “minimum halo” which has no isothermal atmosphere (ground state) and to the quantum core of larger DM halos which have an isothermal atmosphere. For a given value of the core mass M_c , the effect of the BH is to decrease core radius R_c [43].

For noninteracting BECs ($a_s = 0$), the mass-radius relation (12) reduces to

$$M_c = \frac{2\sigma}{\nu} \left(\frac{\hbar^2}{Gm^2 R_c} - \frac{\lambda}{2\sigma} M_{\text{BH}} \right) \quad (14)$$

or, inversely,

$$R_c = \frac{2\sigma}{\nu} \frac{\hbar^2}{Gm^2} \frac{1}{M_c + \frac{\lambda}{\nu} M_{\text{BH}}}. \quad (15)$$

The radius R_c decreases as the mass M_c increases, going from the gravitational Bohr radius⁷

$$R_{\text{B}} = \frac{2\sigma}{\lambda} \frac{\hbar^2}{GM_{\text{BH}} m^2} \quad (16)$$

when $M_c \rightarrow 0$ down to zero when $M_c \rightarrow +\infty$ (see Fig. 3 of [43]). All these configurations are stable. For a given value of the core mass M_c , the core radius decreases as the BH mass increases, going from

$$R_c = \frac{2\sigma}{\nu} \frac{\hbar^2}{Gm^2 M_c} \quad (17)$$

when $M_{\text{BH}} = 0$ to $R_c = R_{\text{B}} \propto M_{\text{BH}}^{-1} \rightarrow 0$ when the BH dominates ($M_{\text{BH}} \rightarrow +\infty$). In the later case, the core

⁶ This relation presents the fundamental scaling $M_h \propto r_h^2$ reflecting the universality of the surface density $\Sigma_0 \sim M_h/r_h^2$ of DM halos [see Eq. (2)].

⁷ When the gravitational attraction of the BH dominates the self-gravity of the quantum core, the GPP equations reduce (in the noninteracting case) to the Schrödinger equation for the hydrogen atom [43].

radius is inversely proportional to the BH mass [see Eq. (16)] rather than the core mass [see Eq. (17)].

We now consider the repulsive case ($a_s > 0$). In the TF limit ($\hbar = 0$), the mass-radius relation (12) reduces to

$$M_c = \frac{-\frac{\lambda}{\nu} M_{\text{BH}}}{1 - \frac{6\pi\zeta a_s \hbar^2}{\nu G m^3 R_c^2}} \quad (18)$$

or, inversely,

$$R_c = \left(\frac{6\pi\zeta}{\nu} \right)^{1/2} \left(\frac{a_s \hbar^2}{G m^3} \right)^{1/2} \frac{1}{\sqrt{1 + \frac{\lambda}{\nu} \frac{M_{\text{BH}}}{M_c}}}. \quad (19)$$

The radius R_c increases as the mass M_c increases, going from $R_c = 0$ when $M_c = 0$ to the TF radius

$$R_{\text{TF}} = \left(\frac{6\pi\zeta}{\nu} \right)^{1/2} \left(\frac{a_s \hbar^2}{G m^3} \right)^{1/2} \quad (20)$$

when $M \rightarrow +\infty$. (see Fig. 4 of [43]). All these configurations are stable. For a given value of the core mass M_c , the core radius decreases as the BH mass increases, going from $R = R_{\text{TF}}$ when $M_{\text{BH}} = 0$ to

$$R_c = \left(\frac{6\pi\zeta}{\lambda} \right)^{1/2} \left(\frac{a_s \hbar^2 M_c}{G m^3 M_{\text{BH}}} \right)^{1/2} \rightarrow 0 \quad (21)$$

when the BH dominates ($M_{\text{BH}} \rightarrow +\infty$). We now consider the general case of a repulsive self-interaction. We must consider two cases. When $M_{\text{BH}} < (M_{\text{BH}})_*$ with

$$(M_{\text{BH}})_* = \frac{2\nu}{\lambda} \left(\frac{\sigma^2}{6\pi\zeta\nu} \right)^{1/2} \frac{\hbar}{\sqrt{Gm|a_s|}}, \quad (22)$$

the radius R_c decreases as the mass M_c increases, going from the gravitational Bohr radius R_B when $M_c \rightarrow 0$ down to the TF radius R_{TF} when $M_c \rightarrow +\infty$ (see Fig. 5 of [43]). When $M_{\text{BH}} > (M_{\text{BH}})_*$, the radius R_c increases as the mass M_c increases, going from the gravitational Bohr radius R_B when $M \rightarrow 0$ up to the TF radius R_{TF} when $M \rightarrow +\infty$ (see Fig. 6 of [43]). All these configurations are stable.

In the attractive case ($a_s < 0$) the mass-radius relation is nonmonotonic (see Fig. 10 of [43]). There is a maximum mass $(M_c)_{\text{max}}(M_{\text{BH}})$ given by

$$\frac{(M_c)_{\text{max}}(M_{\text{BH}})}{(M_c)_{\text{max}}} = -\frac{\lambda}{2\nu} \frac{M_{\text{BH}}}{(M_c)_{\text{max}}} + \sqrt{1 + \frac{\lambda^2}{4\nu^2} \left(\frac{M_{\text{BH}}}{(M_c)_{\text{max}}} \right)^2}, \quad (23)$$

where

$$(M_c)_{\text{max}} = \left(\frac{\sigma^2}{6\pi\zeta\nu} \right)^{1/2} \frac{\hbar}{\sqrt{Gm|a_s|}} \quad (24)$$

is the maximum mass of a self-gravitating BEC with an attractive self-interaction without a central BH [7]. The maximum mass decreases as the mass of the BH increases (see Fig. 11 of [43]). The radius $(R_c)_*(M_{\text{BH}})$ corresponding to $(M_c)_{\text{max}}(M_{\text{BH}})$ is given by

$$\frac{(R_c)_*(M_{\text{BH}})}{(R_c)_*} = \frac{(M_c)_{\text{max}}(M_{\text{BH}})}{(M_c)_{\text{max}}}, \quad (25)$$

where

$$(R_c)_* = \left(\frac{6\pi\zeta}{\nu} \right)^{1/2} \left(\frac{|a_s| \hbar^2}{G m^3} \right)^{1/2} \quad (26)$$

is the radius corresponding to $(M_c)_{\text{max}}$ in the absence of a central BH [7]. No equilibrium state exist with a mass $M_c > (M_c)_{\text{max}}(M_{\text{BH}})$. For $M_c < (M_c)_{\text{max}}(M_{\text{BH}})$ the branch $R_c > (R_c)_*(M_{\text{BH}})$ (corresponding to the solutions (13) with the sign +) is stable while the branch $R_c < (R_c)_*(M_{\text{BH}})$ (corresponding to the solutions (13) with the sign -) is unstable. On the stable branch the radius R_c decreases as the mass M_c increases, going from the gravitational Bohr radius R_B when $M_c \rightarrow 0$ down to the minimum stable radius $(R_c)_*(M_{\text{BH}})$ when $M_c \rightarrow (M_c)_{\text{max}}(M_{\text{BH}})$.

Remark: When $a_s \geq 0$ all the configurations, with any value of M , are stable. Although the central BH enhances the gravitational attraction and reduces the radius of the BEC, it does not destabilize the system. When $a_s < 0$, only the configurations below the maximum mass $(M_c)_{\text{max}}(M_{\text{BH}})$ and above the minimum radius $(R_c)_*(M_{\text{BH}})$ are stable in continuity with the case without central BH [7].

B. The core mass – halo mass relation

Substituting the core mass – radius relation (12) into Eq. (11), we obtain the second degree equation

$$\left(\frac{M_c}{(M_h)_{\text{min},0}} \right)^2 + \frac{\lambda}{\nu} \frac{M_{\text{BH}}}{(M_h)_{\text{min},0}} \frac{M_c}{(M_h)_{\text{min},0}} = \left(\frac{M_h}{(M_h)_{\text{min},0}} \right)^{1/2} \left[1 + \frac{a_s}{a_*} \left(\frac{M_h}{(M_h)_{\text{min},0}} \right)^{1/2} \right] \quad (27)$$

determining the core mass M_c as a function of the halo mass M_h in the presence of a central BH of mass $M_{\text{BH}}(M_h)$ given by Eq. (9). Following our previous paper [16] we have introduced the mass scale

$$(M_h)_{\text{min},0} = \frac{2^{2/3} \sigma^{2/3}}{\nu^{2/3} \alpha^{1/3}} \left(\frac{\hbar^4 \Sigma_0}{G^2 m^4} \right)^{1/3} \quad (28)$$

and the scattering length scale

$$a_* = \frac{2^{2/3} \sigma^{2/3} \alpha^{2/3} \nu^{1/3}}{6\pi\zeta} \left(\frac{G m^5}{\hbar^2 \Sigma_0^2} \right)^{1/3}, \quad (29)$$

where $\alpha = 1/1.76$. Physically $(M_h)_{\min,0}$ gives the minimum mass (ground state) of a noninteracting self-gravitating BEC without central BH. On the other hand, the scattering length a_* determines the transition between the noninteracting regime and the TF regime (for a repulsive self-interaction) or the transition between the noninteracting regime and the collapse regime (for an attractive self-interaction). The solution of Eq. (27) is

$$\frac{M_c}{(M_h)_{\min,0}} = -\frac{\lambda}{2\nu} \frac{M_{\text{BH}}}{(M_h)_{\min,0}} + \left\{ \frac{\lambda^2}{4\nu^2} \left(\frac{M_{\text{BH}}}{(M_h)_{\min,0}} \right)^2 + \left(\frac{M_h}{(M_h)_{\min,0}} \right)^{1/2} \left[1 + \frac{a_s}{a_*} \left(\frac{M_h}{(M_h)_{\min,0}} \right)^{1/2} \right] \right\}^{1/2}. \quad (30)$$

In the absence of BH we recover the relation

$$\frac{M_c}{(M_h)_{\min,0}} = \left(\frac{M_h}{(M_h)_{\min,0}} \right)^{1/4} \sqrt{1 + \frac{a_s}{a_*} \left(\frac{M_h}{(M_h)_{\min,0}} \right)^{1/2}} \quad (31)$$

obtained in [16]. When the BH dominates, we get

$$\frac{M_c}{(M_h)_{\min,0}} = \frac{\nu}{\lambda} \frac{(M_h)_{\min,0}}{M_{\text{BH}}} \left(\frac{M_h}{(M_h)_{\min,0}} \right)^{1/2} \times \left[1 + \frac{a_s}{a_*} \left(\frac{M_h}{(M_h)_{\min,0}} \right)^{1/2} \right]. \quad (32)$$

C. The minimum halo (ground state)

Setting $M_c = M_h$ in Eq. (30) we obtain the minimum halo mass $(M_h)_{\min}$ (ground state) as a function of a_s/a_* in the presence of a central BH. However, for the minimum halo, $M_{\text{BH}}/(M_h)_{\min} \sim 2.51 \times 10^{-5} \ll 1$ and, consequently, we can neglect the effect of the BH. The effect of the BH will be important only for larger halos (see below). Therefore, the results of Secs. VII.B and VII.C of [16] are unchanged. In particular, we obtain the following relation

$$\frac{a_s}{a_*} = \frac{(M_h)_{\min}}{(M_h)_{\min,0}} - \sqrt{\frac{(M_h)_{\min,0}}{(M_h)_{\min}}} \quad (33)$$

between the minimum halo mass $(M_h)_{\min}$ and the scattering length a_s/a_* of the DM particle. This relation is plotted in Fig. 11 of [16]. When $a_s = 0$ we have $(M_h)_{\min} = (M_h)_{\min,0}$. When $a_s \geq 0$, $(M_h)_{\min}$ is larger than $(M_h)_{\min,0}$. When $a_s \leq 0$, $(M_h)_{\min}$ is smaller than $(M_h)_{\min,0}$. When $a_s \geq 0$, the minimum halo is always stable. However, when $a_s < 0$, it is stable only if $M_c < (M_c)_{\max}$ where $(M_c)_{\max}$ is given by [16]:

$$\frac{(M_c)_{\max}}{(M_h)_{\min,0}} = \frac{1}{2} \left(\frac{a_*}{|a_s|} \right)^{1/2}. \quad (34)$$

As a result, the minimum halo is stable provided that $a_s \geq (a_s)_c$ with

$$\frac{(a_s)_c}{a_*} = -\frac{1}{2^{2/3}}. \quad (35)$$

For $a_s = (a_s)_c$, the minimum halo is critical. It has a mass

$$\frac{(M_h)_{\min,c}}{(M_h)_{\min,0}} = \frac{1}{2^{2/3}}. \quad (36)$$

Consequently, for a scattering length $(a_s)_c \leq a_s \leq 0$, the mass of the (stable) minimum halo is in the range $(M_h)_{\min,c} \leq M_h \leq (M_h)_{\min,0}$.

In principle, the minimum halo mass $(M_h)_{\min}$ can be obtained from the observations. Its value is not known precisely but it is of the order of $10^8 M_\odot$ corresponding to dSphs like Fornax. The minimum halo mass $(M_h)_{\min}$ is the only unknown parameter of our theory. In the following, to fix the ideas, we will take

$$(M_h)_{\min} = 10^8 M_\odot. \quad (37)$$

Our formula are general but the numerical applications will slightly change if other, more accurate, values of $(M_h)_{\min}$ are used instead of Eq. (37). We also recall that our approach is approximate because it is based on a Gaussian ansatz for the density profile of DM halos. Again, it could be improved by using the exact core mass-radius relation. However, our main aim in this paper is to present the general ideas, so our approximate analytical approach is sufficient for our purposes.

Once the mass $(M_h)_{\min}$ of the minimum halo is fixed, Eq. (33) determines the relation between the DM particle mass m and the scattering length a_s . This relation can be written as [16]:

$$\frac{a_s}{a'_*} = \left(\frac{m}{m_0} \right)^3 - \frac{m}{m_0}, \quad (38)$$

where we have introduced the particle mass scale

$$m_0 = \frac{2^{1/2} \sigma^{1/2}}{\nu^{1/2} \alpha^{1/4}} \frac{\hbar \Sigma_0^{1/4}}{G^{1/2} (M_h)_{\min}^{3/4}} \quad (39)$$

and the scattering length scale

$$a'_* = \frac{2^{3/2} \sigma^{3/2} \alpha^{1/4}}{\nu^{1/2} 6\pi \zeta} \frac{\hbar}{G^{1/2} \Sigma_0^{1/4} (M_h)_{\min}^{5/4}}. \quad (40)$$

For $(M_h)_{\min} = 10^8 M_\odot$ we obtain

$$m_0 = 2.25 \times 10^{-22} \text{ eV}/c^2 \quad (41)$$

and

$$a'_* = 4.95 \times 10^{-62} \text{ fm}. \quad (42)$$

Physically, m_0 represents the mass of the DM particle in the noninteracting case ($a_s = 0$) which is consistent with a minimum halo of mass $(M_h)_{\min}$. On the other hand, the scattering length a'_* determines the transition between the noninteracting regime and the TF regime (for a repulsive self-interaction) or the transition between the noninteracting regime and the collapse regime (for an

attractive self-interaction). According to Eq. (38), our results depend only on the scattering length a_s of the DM particle: its mass m is then automatically determined by Eq. (38).⁸

The relation (38) is plotted in Fig. 13 of [16]. When $a_s = 0$ we have $m = m_0$. When $a_s \geq 0$, m is larger than m_0 . When $a_s \leq 0$, m is smaller than m_0 . When $a_s \leq 0$, the minimum halo is stable only if $a_s > (a_s)_c$ with

$$\frac{(a_s)_c}{a'_*} = -\frac{1}{2^{3/2}}. \quad (43)$$

For $a_s = (a_s)_c$, the minimum halo is critical. This corresponds to a particle mass

$$\frac{m_c}{m_0} = \frac{1}{\sqrt{2}}. \quad (44)$$

Consequently, for a scattering length $(a_s)_c \leq a_s \leq 0$, the mass of the DM particle is in the range $m_c \leq m \leq m_0$.

Remark: For bosons with an attractive self-interaction, like the axion [12], it is more convenient to express the results in terms of the decay constant (see, e.g., [52])

$$f = \left(\frac{\hbar c^3 m}{32\pi |a_s|} \right)^{1/2}, \quad (45)$$

rather than the scattering length a_s . In that case, the relation (38) can be rewritten as

$$\frac{f}{f'_*} = \frac{1}{\sqrt{1 - \left(\frac{m}{m_0} \right)^2}}, \quad (46)$$

where we have introduced the energy scale [16]:

$$f'_* = \frac{(6\pi\zeta)^{1/2}}{8\pi^{1/2}\sigma^{1/2}\alpha^{1/4}} \hbar^{1/2} \Sigma_0^{1/4} (M_h)_{\min}^{1/4} c^{3/2}. \quad (47)$$

For $(M_h)_{\min} = 10^8 M_\odot$ we obtain

$$f'_* = 9.45 \times 10^{13} \text{ GeV}. \quad (48)$$

The relation (46) is plotted in Fig. 14 of [16]. The minimum halo is stable only if $f > f_c$ with

$$\frac{f_c}{f'_*} = \sqrt{2}. \quad (49)$$

For $f = f_c$, the minimum halo is critical. This corresponds to a particle mass m_c . When $f \rightarrow +\infty$ we have $m \rightarrow m_0$.

D. Procedure to determine the core mass – halo mass relation

In order to determine the core mass – halo mass relation for a given value of the scattering length a_s , we need the following relation [16]

$$\frac{a_s}{a'_*} = \left(\frac{m}{m_0} \right)^{4/3} - \left(\frac{m_0}{m} \right)^{2/3}, \quad (50)$$

which is obtained from Eq. (38) by normalizing the scattering length a_s by the scattering length scale a'_* introduced in Sec. IIIB (see [16] for details). We can now proceed in the following manner. For a given value of a_s/a'_* we can obtain m/m_0 from Eq. (38). Then, we get a_s/a'_* from Eq. (50) and $(M_h)_{\min}/(M_h)_{\min,0}$ from Eq. (33). We can then plot $M_c/(M_h)_{\min}$ as a function of $M_h/(M_h)_{\min}$ by using Eqs. (9) and (30). We stress that this procedure yields a “universal” curve $M_c/(M_h)_{\min}$ vs $M_h/(M_h)_{\min}$ for a given value of a_s/a'_* . The only unknown parameter of our model is the mass $(M_h)_{\min}$ of the minimum halo which determines the scales m_0 and a'_* according to Eqs. (39) and (40).⁹ The minimum halo mass is not known with precision but it is of order $(M_h)_{\min} \sim 10^8 M_\odot$. In the numerical applications, we will assume that $(M_h)_{\min} = 10^8 M_\odot$ [see Eq. (37)]. If we change the value of the minimum halo mass, the normalized curve $M_c/(M_h)_{\min}(M_h/(M_h)_{\min})$ for a given value of a_s/a'_* remains the same: only the scales change.

Remark: For convenience, we have proceeded the other way round. We have fixed a value of $(M_h)_{\min}/(M_h)_{\min,0}$, determined a_s/a'_* from Eq. (33), and plotted $M_c/(M_h)_{\min}$ as a function of $M_h/(M_h)_{\min}$ by using Eqs. (9) and (30). We have then used Eqs. (50) and (38) to obtain the values of m/m_0 and a_s/a'_* corresponding to our choice of $(M_h)_{\min}/(M_h)_{\min,0}$.

E. Noninteracting bosons

For noninteracting bosons ($a_s = 0$), the core mass – halo mass relation (30) reduces to

$$\begin{aligned} \frac{M_c}{(M_h)_{\min}} &= -\frac{\lambda}{2\nu} \frac{M_{\text{BH}}}{(M_h)_{\min}} \\ &+ \sqrt{\frac{\lambda^2}{4\nu^2} \left(\frac{M_{\text{BH}}}{(M_h)_{\min}} \right)^2 + \left(\frac{M_h}{(M_h)_{\min}} \right)^{1/2}}, \end{aligned} \quad (51)$$

where M_{BH} is given as a function of M_h by Eq. (9). More generally, this relation is valid for $|a_s| \ll a'_*$. It is plotted

⁸ Of course, we could take the opposite viewpoint and consider that the scattering length a_s is determined by the mass m so as to be consistent with a minimum halo of mass $(M_h)_{\min}$. However, it is more convenient to take a_s as the control parameter.

⁹ We have also assumed that the surface density of the DM halos is universal [see Eq. (2)]. If this were not the case, our general model would remain valid but the problem would depend on two parameters, M_h and r_h , instead of just M_h .

in Fig. 1. There is a maximum core mass

$$(M_c)_{\max,0} = 8.92 \times 10^8 M_\odot, \quad (52)$$

corresponding to a halo mass

$$(M_h)_{*,0} = 1.96 \times 10^{12} M_\odot \quad (53)$$

and a BH mass

$$(M_{\text{BH}})_{*,0} = 2.39 \times 10^8 M_\odot. \quad (54)$$

The effect of the BH becomes important when $M_{\text{BH}}/(M_h)_{\min} \sim (M_h/(M_h)_{\min})^{1/4}$, i.e. $M_{\text{BH}} \sim M_c$, corresponding to $(M_h)_{*,0} \sim 10^{12} M_\odot$. When $M_h \ll (M_h)_{*,0}$ the effect of the BH is negligible and we recover the scaling

$$\frac{M_c}{(M_h)_{\min}} = \left(\frac{M_h}{(M_h)_{\min}} \right)^{1/4} \quad (55)$$

obtained in [16]. When $M_h \gg (M_h)_{*,0}$ the BH dominates and we get the scaling

$$\begin{aligned} \frac{M_c}{(M_h)_{\min}} &\sim \frac{\nu}{\lambda} \left(\frac{M_h}{(M_h)_{\min}} \right)^{1/2} \frac{(M_h)_{\min}}{M_{\text{BH}}} \\ &\sim \frac{\nu}{\lambda A} \left(\frac{(M_h)_{\min}}{M_h} \right)^{a-1/2}. \end{aligned} \quad (56)$$

This relation can be directly obtained from Eqs. (11) and (16). It exhibits a critical index $a_0 = 1/2$. When $a > a_0$ the core mass decreases with M_h and when $a < a_0$ the core mass increases with M_h . For the measured value $a = 1.16$, we are in the first case. For a DM halo of mass $M_h = 10^{12} M_\odot$ similar to the one that surrounds our Galaxy, we obtain a core mass $M_c = 8.55 \times 10^8 M_\odot$ a little smaller than the value $M_c = 10^9 M_\odot$ obtained in [16] in the absence of a central BH (we have taken $(M_h)_{\min} = 10^8 M_\odot$).

F. Bosons with a repulsive self-interaction

In this section, we consider the case of bosons with a repulsive self-interaction ($a_s > 0$).

We first consider the TF limit corresponding to $a_s \gg a_*$. In that case, the core mass – halo mass relation (30) reduces to

$$\begin{aligned} \frac{M_c}{(M_h)_{\min,0}} &= -\frac{\lambda}{2\nu} \frac{M_{\text{BH}}}{(M_h)_{\min,0}} \\ &+ \sqrt{\frac{\lambda^2}{4\nu^2} \left(\frac{M_{\text{BH}}}{(M_h)_{\min,0}} \right)^2 + \frac{a_s}{a_*} \frac{M_h}{(M_h)_{\min,0}}}. \end{aligned} \quad (57)$$

Substituting the equivalent

$$\frac{(M_h)_{\min}}{(M_h)_{\min,0}} \sim \frac{a_s}{a_*} \quad (58)$$

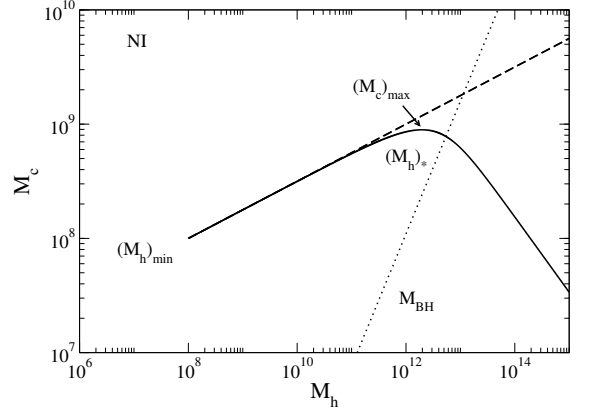


FIG. 1: Core mass M_c as a function of the halo mass M_h (solid line) for noninteracting bosons ($a_s = 0$; $m = m_0 = 2.25 \times 10^{-22} \text{ eV}/c^2$). The mass is normalized by M_\odot . The function $M_c(M_h)$ presents a maximum core mass $(M_c)_{\max,0} = 8.92 \times 10^8 M_\odot$ at $(M_h)_{*,0} = 1.96 \times 10^{12} M_\odot$. All the configurations are stable. We have also represented the relation $M_c(M_h)$ without BH (dashed line) and the relation $M_{\text{BH}}(M_h)$ (dotted line).

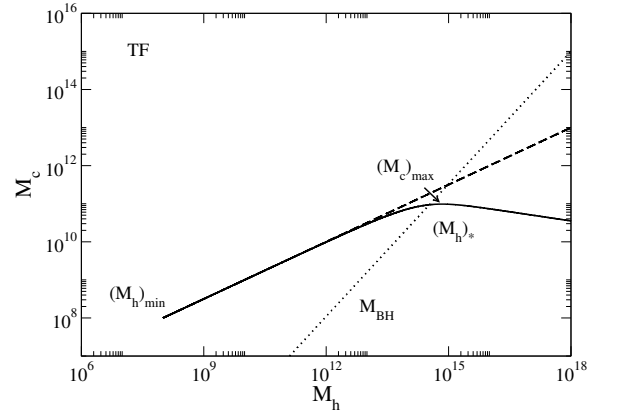


FIG. 2: Core mass M_c as a function of the halo mass M_h (solid line) for a repulsive self-interaction $a_s > 0$ in the TF regime. The mass is normalized by M_\odot . The function $M_c(M_h)$ presents a maximum core mass $(M_c)_{\max,\text{TF}} = 9.77 \times 10^{10} M_\odot$ at $(M_h)_{*,\text{TF}} = 6.92 \times 10^{14} M_\odot$. All the configurations are stable. We have also represented the relation $M_c(M_h)$ without BH (dashed line) and the relation $M_{\text{BH}}(M_h)$ (dotted line).

from Eq. (33) into Eq. (57), we obtain

$$\begin{aligned} \frac{M_c}{(M_h)_{\min}} &= -\frac{\lambda}{2\nu} \frac{M_{\text{BH}}}{(M_h)_{\min}} \\ &+ \sqrt{\frac{\lambda^2}{4\nu^2} \left(\frac{M_{\text{BH}}}{(M_h)_{\min}} \right)^2 + \frac{M_h}{(M_h)_{\min}}}, \end{aligned} \quad (59)$$

where M_{BH} is given as a function of M_h by Eq. (9). This relation is valid for $a_s \gg a'_*$. It is plotted in Fig. 2.

$\frac{(M_h)_{\min}}{(M_h)_{\min,0}}$	$\frac{a_s}{a_*}$	$\frac{m}{m_0}$	$\frac{a_s}{a'_*}$	$\frac{(M_c)_{\max}}{(M_h)_{\min}}$	$\frac{(M_h)_*}{(M_h)_{\min}}$
10^4	10^4	10^3	10^9	977	6.92×10^6
1.6	0.809	1.42	1.46	537	4.12×10^6
1.1	0.1465	1.07	0.165	167	1.48×10^6
1.01	0.015	1.01	0.01515	26.8	2.23×10^5
1	0	1	0	8.92	1.96×10^4

TABLE I: Values of the DM particle parameters selected in Fig. 3. The scales m_0 and a'_* are given by Eqs. (39) and (40). For $(M_h)_{\min} = 10^8 M_\odot$, we obtain $m_0 = 2.25 \times 10^{-22} \text{ eV}/c^2$ and $a'_* = 4.95 \times 10^{-62} \text{ fm}$.

There is a maximum core mass

$$(M_c)_{\max, \text{TF}} = 9.77 \times 10^{10} M_\odot, \quad (60)$$

corresponding to a halo mass

$$(M_h)_{*, \text{TF}} = 6.92 \times 10^{14} M_\odot \quad (61)$$

and a BH mass

$$(M_{\text{BH}})_{*, \text{TF}} = 2.16 \times 10^{11} M_\odot. \quad (62)$$

The effect of the BH becomes important when $M_{\text{BH}}/(M_h)_{\min} \sim (M_h/(M_h)_{\min})^{1/2}$, i.e. $M_{\text{BH}} \sim M_c$, corresponding to $(M_h)_{*, \text{TF}} \sim 10^{15} M_\odot$.¹⁰ When $M_h \ll (M_h)_{*, \text{TF}}$ the effect of the BH is negligible we recover the scaling

$$\frac{M_c}{(M_h)_{\min}} = \left(\frac{M_h}{(M_h)_{\min}} \right)^{1/2} \quad (63)$$

obtained in [16]. When $M_h \gg (M_h)_{*, \text{TF}}$, the BH dominates and we get the scaling

$$\begin{aligned} \frac{M_c}{(M_h)_{\min}} &\sim \frac{\nu}{\lambda} \frac{M_h}{(M_h)_{\min}} \frac{(M_h)_{\min}}{M_{\text{BH}}} \\ &\sim \frac{\nu}{\lambda A} \left(\frac{(M_h)_{\min}}{M_h} \right)^{a-1}. \end{aligned} \quad (64)$$

This relation can be directly obtained from Eqs. (11) and (21). It exhibits a critical index $a_{\text{TF}} = 1$. When $a > a_{\text{TF}}$ the core mass decreases with M_h and when $a < a_{\text{TF}}$ the core mass increases with M_h . For the measured value $a = 1.16$ we are in the first case. But since $a = 1.16$ is close to the critical value $a_{\text{TF}} = 1$, the decrease of the core mass M_c with M_h is weak, as can be seen in Fig. 2. For a DM halo of mass $M_h = 10^{12} M_\odot$ similar to the one that surrounds our Galaxy, we obtain a core mass $M_c = 10^{10} M_\odot$, the same value as the one found in [16] in the absence of a central BH (we have taken $(M_h)_{\min} = 10^8 M_\odot$).

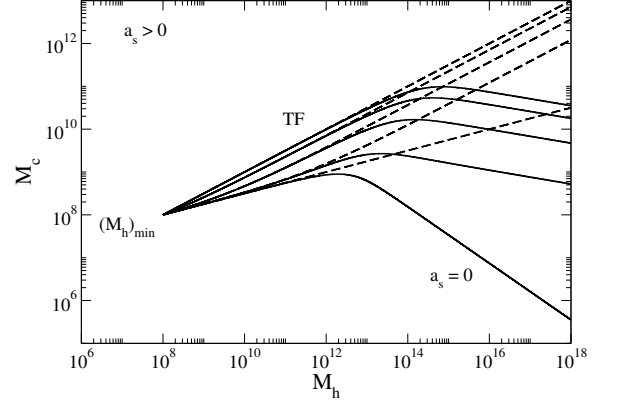


FIG. 3: Core mass M_c as a function of the halo mass M_h for different values of the scattering length $a_s \geq 0$ (see Table I). The mass is normalized by M_\odot . We have represented the position of the minimum halo mass $(M_h)_{\min} = 10^8 M_\odot$ (common origin), the curve corresponding to noninteracting bosons $a_s = 0$ [see Eq. (51)], and the curve corresponding to the TF limit $a_s/a'_* \gg 1$ [see Eq. (59)]. The core mass reaches a maximum value $(M_c)_{\max}$ at $(M_h)_*$. The dashed line represents the core mass – halo mass relation $M_c(M_h)$ in the absence of a central BH [16]. In that case, the core mass increases monotonically with the halo mass.

We now consider the general case of a repulsive self-interaction ($a_s > 0$). The core mass – halo mass relation $M_c(M_h)$ is represented in Fig. 3 for different values of a_s following the procedure explained in Sec. III D. These curves are bounded by the lower curve from Eq. (51) corresponding to the noninteracting limit ($a_s \ll a'_*$) and by the upper curve from Eq. (59) corresponding to the TF limit ($a_s \gg a'_*$). The general behavior of the function $M_c(M_h)$ is always the same. Starting from the minimum halo mass $(M_h)_{\min}$ where $M_c = M_h$, the core mass M_c increases with M_h , reaches a maximum $(M_c)_{\max}$ at $(M_h)_*$, and finally decreases with M_h . All the halos are stable. We see that the maximum mass $(M_c)_{\max}$ increases with a_s going from $(M_c)_{\max,0} = 8.92 \times 10^8 M_\odot$ for $a_s = 0$ to $(M_c)_{\max, \text{TF}} = 9.77 \times 10^{10} M_\odot$ for $a_s/a'_* \gg 1$. The corresponding halo mass $(M_h)_*$ increases with a_s going from $(M_h)_{*,0} = 1.96 \times 10^{12} M_\odot$ to $(M_h)_{*, \text{TF}} = 6.92 \times 10^{14} M_\odot$. The effect of the BH is negligible for small halo masses $M_h \ll (M_h)_*$. It becomes important when $M_h \sim (M_h)_*$.

¹⁰ Since the value of $(M_h)_{*, \text{TF}}$ is larger than the size of the biggest DM halos in the Universe, we conclude that the effect of the BH is always negligible (or marginal for the biggest halos) when we are in the TF limit.

G. Bosons with an attractive self-interaction

In this section, we consider the case of bosons with an attractive self-interaction ($a_s < 0$).

According to Eq. (30) the core mass vanishes at

$$\frac{(M_h)_{\text{Max}}}{(M_h)_{\text{min},0}} = \left(\frac{a_*}{a_s} \right)^2, \quad (65)$$

like in the absence of a central BH [16]. However, this situation is purely academic because, as we shall see, the core becomes unstable long before disappearing.

The core mass – halo mass relation $M_c(M_h)$ is plotted in Fig. 4 for a given value of $a_s < 0$. The function $M_c(M_h)$ presents a maximum $(M_c)_{\text{max}}$ at $(M_h)_*$. It is important to note that the maximum of the function $M_c(M_h)$ does *not* generally coincide with the maximum mass $(M_c)_{\text{max},*}$ of the quantum core in the presence of a BH of mass M_{BH} [see Eq. (23)]. The evolution of the critical mass $(M_c)_{\text{max},*}$ with M_h is determined by the equation¹¹

$$\begin{aligned} \frac{(M_c)_{\text{max},*}}{(M_h)_{\text{min},0}} &= -\frac{\lambda}{2\nu} \frac{M_{\text{BH}}}{(M_h)_{\text{min},0}} \\ &+ \sqrt{\frac{\lambda^2}{4\nu^2} \left(\frac{M_{\text{BH}}}{(M_h)_{\text{min},0}} \right)^2 + \frac{1}{4} \frac{a_*}{|a_s|}}, \quad (67) \end{aligned}$$

together with Eq. (9). The intersection between the curves $(M_c)(M_h)$ and $(M_c)_{\text{max},*}(M_h)$ determines the point $((M_h)_{\text{max}}, (M_c)_{\text{crit}})$ at which the core of the halo becomes unstable (it is marginally stable at that point). The branch $(M_h)_{\text{max}} \leq M_h \leq (M_h)_{\text{Max}}$ corresponds to unstable states. Only the branch $(M_h)_{\text{min}} \leq M_h \leq (M_h)_{\text{max}}$, corresponding to stable states, is physical. Therefore, $(M_h)_{\text{max}}$ is the maximum mass of a DM halo with a stable quantum core.

We now consider the general case of an attractive self-interaction ($a_s < 0$). The core mass – halo mass relation $M_c(M_h)$ is represented in Figs. 5 and 6 for different values of a_s in the range $[(a_s)_c, 0]$ following the procedure explained in Sec. III D. These curves are bounded by the lower curve $(M_h)_{\text{min}} = (M_h)_{\text{max}}$ (critical minimum halo) corresponding to the minimum scattering length $(a_s)_c$ and by the upper curve from Eq. (51) corresponding to the noninteracting limit ($|a_s| \ll a'_*$). The general behavior of the $M_c(M_h)$ relation is always the same. Starting from the minimum halo mass $(M_h)_{\text{min}}$ where $M_c = M_h$, the core mass M_c increases with M_h , reaches a maximum at $(M_c)_{\text{max}}$ at $(M_h)_*$ and finally decreases with M_h . The halos are stable until $(M_h)_{\text{max}}$ corresponding

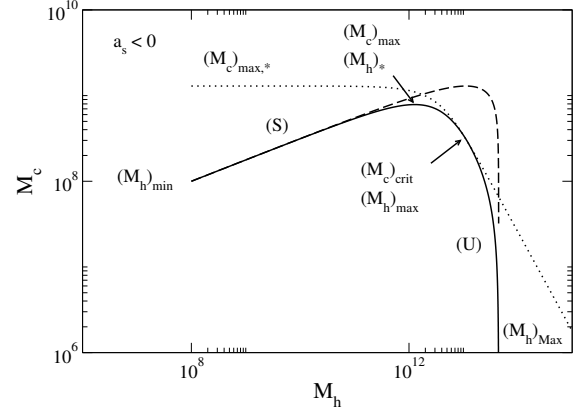


FIG. 4: Core mass M_c as a function of the halo mass M_h for a specific value of $a_s < 0$ (we have taken $a_s/a'_* = -0.00150$). The core mass reaches a maximum value $(M_c)_{\text{max}}$ at $(M_h)_*$. However, the DM halo is stable until the maximum halo mass $(M_h)_{\text{max}}$ corresponding to a critical core mass $(M_c)_{\text{crit}}$ [see Eq. (23)]. The dashed line represents the core mass – halo mass relation $M_c(M_h)$ without a central BH. The dotted line represents the maximum mass of the core in the presence of a BH of mass $M_{\text{BH}}(M_h)$.

to $M_c = (M_c)_{\text{crit}}$. For $M_h > (M_h)_{\text{max}}$ they are unstable. For $M_h = (M_h)_{\text{Max}}$ the core mass vanishes ($M_c = 0$). We see that the maximum mass $(M_c)_{\text{max}}$ increases with a_s , going from $(M_h)_{\text{min}} = 10^8 M_\odot$ for $a_s = (a_s)_c$ to $(M_c)_{\text{max},0} = 8.92 \times 10^8 M_\odot$ for $a_s = 0$. The corresponding halo mass $(M_h)_*$ increases with a_s going from $(M_h)_{\text{min}} = 10^8 M_\odot$ to $(M_h)_{*,0} = 1.96 \times 10^{12} M_\odot$.¹² On the other hand, the critical mass $(M_c)_{\text{crit}}$ decreases with a_s going from $(M_h)_{\text{min}} = 10^8 M_\odot$ for $a_s = (a_s)_c$ to 0 for $a_s = 0$ while the maximum halo mass $(M_h)_{\text{max}}$ increases with a_s going from $(M_h)_{\text{min}} = 10^8 M_\odot$ to $+\infty$. The effect of the BH is negligible for a_s close to $(a_s)_c$. In that case $(M_c)_{\text{crit}} \simeq (M_c)_{\text{max}}$ and $(M_h)_{\text{max}} \simeq (M_h)_*$. It is also negligible for any a_s when $M_h \ll (M_h)_*$. It becomes important when a_s is close to 0 and $M_h \sim (M_h)_*$.

H. Summary

In the noninteracting case ($a_s = 0$; $m = m_0$ given by Eq. (41)) the DM halos with a mass $M_h \geq (M_h)_{\text{min}}$ [see Eq. (37)] contain a quantum core of mass M_c given by Eq. (51). The core mass achieves a maximum value $(M_c)_{\text{max},0}$ at $(M_h)_{*,0}$ [see Eqs. (52) and (53)]. All the configurations are stable.

In the case of a repulsive self-interaction ($a_s > 0$; $m > m_0$ given by Eq. (38)) the halos with a mass

¹¹ This equation is obtained by combining Eq. (23) with the relation

$$\frac{(M_c)_{\text{max}}}{(M_h)_{\text{min},0}} = \frac{1}{2} \left(\frac{a_*}{|a_s|} \right)^{1/2} \quad (66)$$

given in [16] in the absence of a central BH.

¹² This is very different from the case without a central BH where the maximum core mass and the corresponding halo mass increase to infinity when a_s goes to 0⁻ [16].

$\frac{(M_h)_{\min}}{(M_h)_{\min,0}}$	$\frac{a_s}{a_*}$	$\frac{m}{m_0}$	$\frac{a_s}{a'_*}$	$\frac{f}{f'_*}$	$\frac{(M_h)_*}{(M_h)_{\min}}$	$\frac{(M_c)_{\max}}{(M_h)_{\min}}$	$\frac{(M_h)_{\max}}{(M_h)_{\min}}$	$\frac{(M_c)_{\text{crit}}}{(M_h)_{\min}}$
1	0	1	0	∞	1.96×10^4	8.92	∞	0
0.9999	-1.50×10^{-4}	1.00	-1.50×10^{-4}	81.6	1.88×10^4	8.81	1.11×10^7	0.158
0.999	-1.50×10^{-3}	0.999	-0.00150	25.8	1.27×10^4	7.85	1.11×10^5	3.11
0.995	-0.00751	0.996	-0.00746	11.55	3040	5.33	4460	5.22
0.98	-0.03015	0.985	-0.0294	5.79	270	2.91	281	2.91
0.95	-0.0760	0.962	-0.0713	3.67	45.6	1.91	45.6	1.91
0.9	-0.154	0.924	-0.135	2.615	11.7	1.41	11.7	1.41
0.8	-0.318	0.846	-0.241	1.87	3.09	1.11	3.09	1.11
0.630	-0.630	0.707	-0.354	1.41	1	1	1	1

TABLE II: Values of the DM particle parameters selected in Figs. 5 and 6. The scales m_0 , a'_* and f'_* are given by Eqs. (39), (40) and (47). For $(M_h)_{\min} = 10^8 M_\odot$, we obtain $m_0 = 2.25 \times 10^{-22} \text{ eV}/c^2$, $a'_* = 4.95 \times 10^{-62} \text{ fm}$ and $f'_* = 9.45 \times 10^{13} \text{ GeV}$.

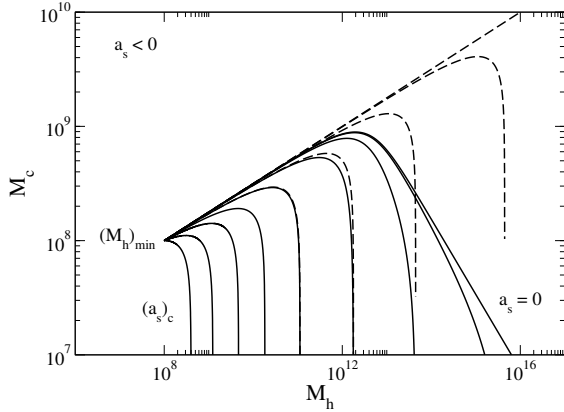


FIG. 5: Core mass M_c as a function of the halo mass M_h for different values of the scattering length $(a_s)_c \leq a_s \leq 0$ (see Table II). The mass is normalized by M_\odot . We have represented the position of the minimum halo mass $(M_h)_{\min} = 10^8 M_\odot$ (common origin), the curve corresponding to the minimum scattering length $(a_s)_c$ for which the minimum halo is critical, and the curve corresponding to noninteracting bosons $a_s = 0$ [see Eq. (51)]. The core mass reaches a maximum value $(M_c)_{\max}$ at $(M_h)_*$. The dashed lines represent the core mass – halo mass relation $M_c(M_h)$ in the absence of a central BH [16].

$M_h > (M_h)_{\min}$ [see Eq. (37)] contain a quantum core of mass M_c given by Eq. (30). The core mass achieves a maximum value $(M_c)_{\max}$ at $(M_h)_*$. For $a_s \ll a_*$, we are in the noninteracting limit discussed previously. For $a_s \gg a_*$ we are in the TF limit. In that case, the mass M_c of the quantum core is given by Eq. (59). The core mass achieves a maximum value $(M_c)_{\max, \text{TF}}$ at $(M_h)_{*, \text{TF}}$ [see Eqs. (60) and (61)]. All the configurations are stable.

In the case of an attractive self-interaction ($a_s < 0$) the halos can be stable only if $a_s > (a_s)_c$ (or equivalently $f > f_c$). When $(a_s)_c \leq a_s < 0$ (correspondingly $m_c \leq m < m_0$ given by Eq. (38)) the halos with a mass $M_h > (M_h)_{\min}$ [see Eq. (37)] contain a quantum core of mass M_c given by Eq. (30). The core mass achieves a

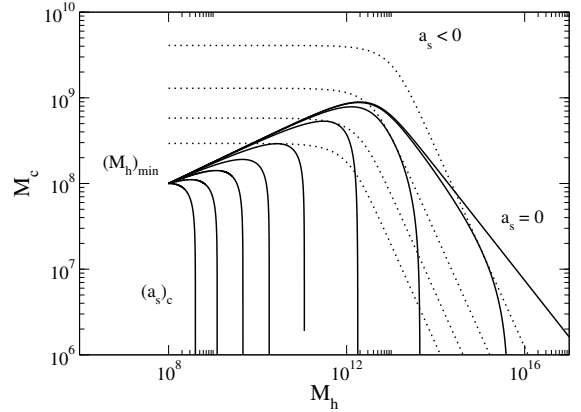


FIG. 6: Same as Fig. 5 but now the dotted lines represent the maximum mass of the quantum core $(M_c)_{\max,*}(M_h)$ in the presence of a BH of mass $M_{\text{BH}}(M_h)$. Their intersections with the core mass – halo mass relations $M_c(M_h)$ (solid lines) determine the points $((M_h)_{\max}, (M_c)_{\text{crit}})$ at which the core of the halo becomes unstable. For values of a_s close to $(a_s)_c$ we have not plotted the dotted lines because $(M_c)_{\max}$ and $(M_c)_{\text{crit}}$ coincide. When $a_s < (a_s)_c$ (i.e. $f < f_c$) there is no DM halo with a stable quantum core. When $(a_s)_c < a_s < 0$ a stable quantum core exists only in the range $(M_h)_{\min} \leq M_h \leq (M_h)_{\max}$.

maximum value $(M_c)_{\max}$ at $(M_h)_*$. The quantum core is stable for $(M_h)_{\min} < M_h < (M_h)_{\max}$ and unstable for $(M_h)_{\max} < M_h < (M_h)_{\text{Max}}$. When we reach the maximum halo mass $(M_h)_{\max}$, the core reaches its maximum limit $(M_c)_{\text{crit}}$ [see Eq. (23)] and collapses. The result of the collapse (dense axion star, BH, bosonova...) is discussed in [52–60].

The maximum core mass $(M_c)_{\max}$ and the critical core mass $(M_c)_{\text{crit}}$ are plotted as a function of a_s in Fig. 7. The corresponding halo masses $(M_h)_*$ and $(M_h)_{\max}$ are plotted as a function of a_s in Fig. 8.

In the previous sections, we have expressed the core mass – halo mass relation in terms of M_h . This relation can be easily expressed in terms of M_v by using Eq. (6).

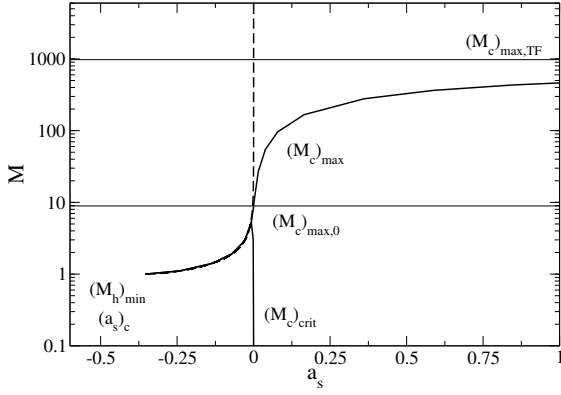


FIG. 7: Maximum core mass $(M_c)_{\max}/(M_h)_{\min}$ and critical core mass $(M_c)_{\text{crit}}/(M_h)_{\min}$ as a function of the scattering length a_s/a_* . For $a_s \geq 0$, the critical core mass $(M_c)_{\text{crit}} = 0$ meaning that all the configurations are stable. The dashed line represents the maximum core mass $(M_c)_{\max}/(M_h)_{\min}$ in the absence of a central BH [see Eq. (239) of [16]] which tends to $+\infty$ as $a_s \rightarrow 0^-$.

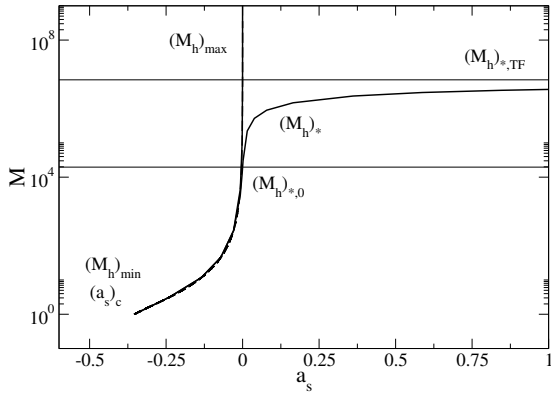


FIG. 8: Halo mass $(M_h)_*/(M_h)_{\min}$ corresponding to the maximum core mass and maximum halo mass $(M_h)_{\max}/(M_h)_{\min}$ above which the quantum core is unstable as a function of the scattering length a_s/a_* . For $a_s \geq 0$, the maximum halo mass $(M_h)_{\max} = +\infty$ meaning that all the configurations are stable. The dashed line represents the maximum halo mass $(M_h)_{\max}/(M_h)_{\min}$ in the absence of a central BH [see Eq. (238) of [16]].

IV. FERMIONIC DM HALOS

In this section, we obtain the core mass – halo mass relation of fermionic DM halos in the presence of a central BH by combining the velocity dispersion tracing relation (11) with the core mass-radius relation of a self-gravitating gas of fermions at $T = 0$.

A. Core mass-radius relation

Using a Gaussian ansatz, we found in [43] that the approximate mass-radius relation of a self-gravitating gas of fermions at $T = 0$ (ground state) with a central BH is given by

$$R_c = \frac{3\zeta}{20} \left(\frac{3}{\pi}\right)^{2/3} \frac{h^2}{Gm^{8/3}} \frac{M_c^{2/3}}{\nu M_c + \lambda M_{\text{BH}}} \quad (68)$$

with the coefficients $\zeta = 1/(2\pi)^{3/2}$, $\nu = 1/\sqrt{2\pi}$ and $\lambda = 2/\sqrt{\pi}$. These results apply to the “minimum halo” which has no isothermal atmosphere (ground state) and to the quantum core of larger DM halos which have an isothermal atmosphere. Starting from $R_c = 0$ when $M_c = 0$, the radius R_c increases as the mass M_c increases, reaches a maximum

$$(R_c)_{\max}(M_{\text{BH}}) = \frac{\zeta}{20\lambda^{1/3}} \left(\frac{6}{\pi\nu}\right)^{2/3} \frac{h^2}{Gm^{8/3} M_{\text{BH}}^{1/3}} \quad (69)$$

at

$$M_*(M_{\text{BH}}) = \frac{2\lambda}{\nu} M_{\text{BH}} \quad (70)$$

and decreases to zero when $M \rightarrow +\infty$ (see Fig. 18 of [43]). All these configurations are stable. For a given value of the core mass M_c , the core radius decreases as the BH mass increases going from

$$R_c = \frac{3\zeta}{20\nu} \left(\frac{3}{\pi}\right)^{2/3} \frac{h^2}{Gm^{8/3} M_c^{1/3}} \quad (71)$$

when $M_{\text{BH}} = 0$ to

$$R_c \sim \frac{3\zeta}{20\lambda} \left(\frac{3}{\pi}\right)^{2/3} \frac{h^2 M_c^{2/3}}{Gm^{8/3} M_{\text{BH}}} \rightarrow 0 \quad (72)$$

when the BH dominates ($M_{\text{BH}} \rightarrow +\infty$). Although the central BH enhances the gravitational attraction and reduces the radius of the BEC, it does not destabilize the system.

B. The minimum halo mass without central BH

We first determine the minimum halo mass $(M_h)_{\min}$ in the absence of a central BH. As explained previously, the minimum halo corresponds to the ground state ($T = 0$) of the self-gravitating Fermi gas. In our approximate approach we write the surface density as

$$\Sigma_0 = \alpha \frac{M_c}{R_c^2}, \quad (73)$$

where α is a constant of order unity (in the numerical applications we take $\alpha = 1/1.76$ for the reason explained in footnote 17 of [16]). Eliminating R_c between Eqs. (71)

and (73), and treating Σ_0 as a universal constant, we get the minimum halo mass $(M_h)_{\min}$ as a function of m (we recall that $M_h = M_c$ for the ground state since there is no isothermal atmosphere by definition). We find

$$(M_h)_{\min} = \frac{(2\pi)^{12/5}}{\alpha^{3/5}\nu^{6/5}} \left(\frac{3\zeta}{20}\right)^{6/5} \left(\frac{3}{\pi}\right)^{4/5} \left(\frac{\hbar^{12}\Sigma_0^3}{G^6 m^{16}}\right)^{1/5}. \quad (74)$$

The prefactor is 1.26. This result can be compared with the exact value from Eq. (14) of [16]. Measuring the DM particle mass in units of $100 \text{ eV}/c^2$, we get $(M_h)_{\min} = 1.40 \times 10^8 m^{-16/5} M_\odot$. Inversely, assuming that the mass $(M_h)_{\min}$ of the minimum halo is known, we obtain the fermion mass

$$m = \frac{(2\pi)^{3/4}}{\alpha^{3/16}\nu^{3/8}} \left(\frac{3\zeta}{20}\right)^{3/8} \left(\frac{3}{\pi}\right)^{1/4} \frac{\hbar^{3/4}\Sigma_0^{3/16}}{G^{3/8}(M_h)_{\min}^{5/16}}. \quad (75)$$

The prefactor is 1.07. If we take $(M_h)_{\min} = 10^8 M_\odot$ we obtain $m = 111 \text{ eV}/c^2$. This result can be compared with the exact value from Eq. (G12) of [16].

C. The core mass – halo mass relation without central BH

Substituting the core mass-radius relation (71) into Eq. (11), we obtain the core mass – halo mass relation without central BH

$$\frac{M_c}{(M_h)_{\min}} = \left(\frac{M_h}{(M_h)_{\min}}\right)^{3/8}. \quad (76)$$

We recover the scaling from Eq. (169) of [16]. Returning to the original variables, we get

$$M_c = \frac{(2\pi)^{3/2}}{\alpha^{3/8}\nu^{3/4}} \left(\frac{3\zeta}{20}\right)^{3/4} \left(\frac{3}{\pi}\right)^{1/2} \left(\frac{\hbar^4 \Sigma_0 M_h}{G^2 m^{16/3}}\right)^{3/8}. \quad (77)$$

The prefactor is 1.155. For a DM halo of mass $M_h = 10^{12} M_\odot$ similar to the one that surrounds our Galaxy, we obtain a core mass $M_c = 3.16 \times 10^9 M_\odot$ (we have taken $(M_h)_{\min} = 10^8 M_\odot$). The corresponding core radius is $R_c = 201 \text{ pc}$ [see Eq. (71)]. The quantum core represents a bulge or a nucleus (it cannot mimic a BH).

D. The core mass – halo mass relation with a central BH

We now take into account the presence of a central BH. Substituting the core mass-radius relation (68) into Eq. (11), we obtain the equation

$$\left[\frac{M_c}{(M_h)_{\min}} + \frac{\lambda}{\nu} \frac{M_{\text{BH}}}{(M_h)_{\min}} \right] \left(\frac{M_c}{(M_h)_{\min}} \right)^{1/3} = \left(\frac{M_h}{(M_h)_{\min}} \right)^{1/2} \quad (78)$$

determining the core mass M_c as a function of the halo mass M_h in the presence of a central BH of mass $M_{\text{BH}}(M_h)$ given by Eq. (9). We have introduced the mass scale from Eq. (74) corresponding to the minimum halo mass without central BH. Setting $M_c = M_h$ in Eq. (78) we obtain the minimum halo mass $(M_h)_{\min}(M_{\text{BH}})$ in the presence of a central BH. However, we have already explained in Sec. III C that we can neglect the effect of the BH on the minimum halo. The effect of the BH will be important only for larger halos (see below). Therefore, the minimum halo mass in the presence of a central BH is still given in very good approximation by Eq. (74).

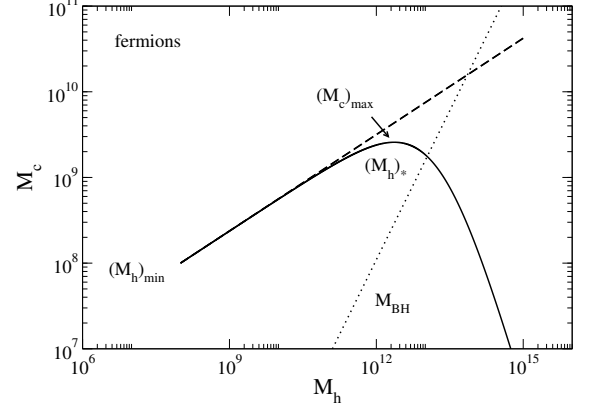


FIG. 9: Core mass M_c as a function of the halo mass M_h (solid line) for fermions ($m = 111 \text{ eV}/c^2$). The mass is normalized by M_\odot . The function $M_c(M_h)$ presents a maximum core mass $(M_c)_{\text{max},F} = 2.57 \times 10^9 M_\odot$ at $(M_h)_{*,F} = 2.31 \times 10^{12} M_\odot$. All the configurations are stable. We have also represented the relation $M_c(M_h)$ without BH (dashed line) and the relation $M_{\text{BH}}(M_h)$ (dotted line).

The core mass – halo mass relation (78) is plotted in Fig. 9. There is a maximum core mass

$$(M_c)_{\text{max},F} = 2.57 \times 10^9 M_\odot, \quad (79)$$

corresponding to a halo mass

$$(M_h)_{*,F} = 2.31 \times 10^{12} M_\odot \quad (80)$$

and a BH mass

$$(M_{\text{BH}})_{*,F} = 2.89 \times 10^8 M_\odot. \quad (81)$$

The effect of the BH becomes important when $M_{\text{BH}} \sim M_c$, corresponding to $(M_h)_{*,F} \sim 10^{12} M_\odot$. When $M_h \ll (M_h)_*$ the effect of the BH is negligible and we recover the scaling

$$\frac{M_c}{(M_h)_{\min}} \sim \left(\frac{M_h}{(M_h)_{\min}} \right)^{3/8} \quad (82)$$

corresponding to Eq. (76).

When $M_h \gg (M_h)_*$ the BH dominates and we get the scaling

$$\begin{aligned} \frac{M_c}{(M_h)_{\min}} &\sim \left(\frac{\nu}{\lambda}\right)^3 \left(\frac{(M_h)_{\min}}{M_{\text{BH}}}\right)^3 \left(\frac{M_h}{(M_h)_{\min}}\right)^{3/2} \\ &\sim \left(\frac{\nu}{\lambda}\right)^3 \frac{1}{A^3} \left(\frac{(M_h)_{\min}}{M_h}\right)^{3a-3/2}. \end{aligned} \quad (83)$$

This relation can be directly obtained from Eqs. (11) and (72). It exhibits a critical index $a_F = 1/2$. When $a > a_F$ the core mass decreases with M_h and when $a < a_F$ the core mass increases with M_h . For the measured value $a = 1.16$, we are in the first case. For a DM halo of mass $M_h = 10^{12} M_\odot$ similar to the one that surrounds our Galaxy, we obtain a core mass $M_c = 2.39 \times 10^9 M_\odot$ a little smaller than the value $M_c = 3.16 \times 10^9 M_\odot$ obtained above in the absence of a central BH (we have taken $(M_h)_{\min} = 10^8 M_\odot$).

E. Summary

In the fermion case ($m = 111 \text{ eV}/c^2$ given by Eq. (75)) the halos with a mass $M_h \geq (M_h)_{\min}$ [see Eq. (74)] contain a quantum core of mass M_c given by Eq. (78). The core mass achieves a maximum value $(M_c)_{\max, F}$ at $(M_h)_{*, F}$ [see Eqs. (79) and (80)]. All the configurations are stable.

In this section, we have expressed the core mass – halo mass relation in terms of M_h . This relation could be easily expressed in terms of M_v by using Eq. (6).

V. COMPARISON WITH OTHER WORKS

Let us briefly compare our results with those obtained by Davies and Mocz [44]. These authors consider fuzzy DM soliton cores made of noninteracting bosons around SMBHs and assume that the $M_c(M_h)$ relation is unchanged by the presence of the SMBH. If we take into account the effect of the SMBH in the manner performed in the present paper, we find that, for noninteracting bosons, the effect of the BH becomes important for DM halos of mass $(M_h)_{*, 0} = 1.96 \times 10^{12} M_\odot$. Accordingly, for the DM halos considered by Davies and Mocz [44], with mass $M_v = 10^{12} M_\odot$ (Milky Way) and $M_v = 2 \times 10^{14} M_\odot$ (elliptical galaxy in the Virgo cluster), the presence of the SMBH is expected to change the value of the core mass (especially in the second case), except if it forms after the quantum core as assumed by these authors.¹³

The same conclusion is reached in the case of fermions for which $(M_h)_{*, F} = 2.31 \times 10^{12} M_\odot$. By contrast, for self-interacting bosons in the TF limit, we find that the effect of the BH becomes important for DM halos of mass $(M_h)_{*, TF} = 6.92 \times 10^{14} M_\odot$. This mass scale is of the order of the mass of the largest DM halos in the Universe. As a result, for most DM halos made of self-interacting bosons in the TF limit, the effect of the SMBH is negligible, or only marginally important. Finally, for bosons with a repulsive self-interaction, the effect of the BH is negligible when a_s is close to $(a_s)_c$ while it becomes important for halos of size $M_h \sim 10^{12} M_\odot$ when a_s is close to zero. From Fig. 5 and Table II (which can be compared with Table I of [16]) we see that the transition occurs for $a_s/a'_* \sim -0.00746$ (with $a'_* = 4.95 \times 10^{-62} \text{ fm}$).

VI. CONCLUSION

In this paper, we have analytically derived the core mass – halo mass relation of bosonic and fermionic DM halos in the presence of a central BH. Our results are summarized in Secs. III H (for bosons) and IV E (for fermions). They generalize the results previously reported in [16] in the case without central BH. To obtain our results, we have used the BH mass – halo mass relation (3) obtained from the observations [51], the core mass – radius relations (12) and (68) in the presence of a central BH obtained from a Gaussian ansatz in [43], and the velocity dispersion tracing relation (10) introduced in [8, 26, 37] and justified from an effective thermodynamic approach in [8, 16]. We have assumed that this relation remains valid in the presence of a central BH. We have also assumed that the BH exists prior to the quantum core and that it affects its mass-radius relation in the manner discussed in [43]. However, very little is known about the mechanism of formation of SMBHs at the center of galaxies. It could well be that the SMBH is formed after the quantum core, and could even result from its gravitational collapse. In this respect, we have argued in [8, 16] that above a critical halo mass $(M_h)_{\text{MCP}}$, related to a microcanonical critical point in our effective thermodynamic model, the core-halo structure of DM halos becomes unstable. In that case, the system undergoes a gravothermal catastrophe followed by a dynamical instability of general relativistic origin [42] leading to the formation of a SMBH. This could be a manner to form SMBHs at the center of galaxies, although our arguments

their Fig. 1) assume that the BECDM particle is noninteracting. As emphasized in our series of papers [7, 8, 15, 16], and recalled in the Introduction, the consideration of a self-interaction can considerably change the value of the DM particle mass, up to 20 orders of magnitude, and solve some tensions with observations. The possibility of a self-interaction should be taken into account in the literature when considering astrophysical constraints on the BECDM particle mass.

¹³ As discussed by Davies and Mocz [44] at the end of their Sec. 4, their conclusions are robust and should not significantly change if we properly account for the modification of the quantum core mass due to the presence of the SMBH as suggested above. We stress, however, that their results (and all the results quoted in

suggest that this scenario works only for sufficiently large halos ($M_h \gtrsim 10^{11} M_\odot$). [Actually, the fact that SMBHs can form only in sufficiently large galaxies is consistent with the conclusion reached by Ferrarese [50] on the basis of observations.] Therefore, different mechanisms of SMBH formation at the center of galaxies are possible. They should be investigated in future works.

Appendix A: The case of a fixed BH mass

In main text, when studying the core mass – halo mass relation $M_c(M_h)$, we have taken into account the dependence of the BH mass with the halo mass [see Eq. (9)]. This is the astrophysically relevant situation. However, it is interesting to consider, for comparison, the behavior of the core mass – halo mass relation $M_c(M_h)$ in the academic case where the BH mass is fixed. This relation

is determined by Eq. (27) or Eq. (30), where M_{BH} is now a constant. When $a_s \geq 0$, the function $M_c(M_h)$ is monotonic. When $a_s < 0$, the core mass is maximum at

$$\frac{(M_h)_{\text{max}}^{\text{fixedBH}}}{(M_h)_{\text{min},0}} = \frac{1}{4} \left(\frac{a_*}{a_s} \right)^2 \quad (\text{A1})$$

as in the absence of a central BH [16]. It has the the value

$$\begin{aligned} \frac{(M_c)_{\text{max}}^{\text{fixedBH}}}{(M_h)_{\text{min},0}} &= -\frac{\lambda}{2\nu} \frac{M_{\text{BH}}}{(M_h)_{\text{min},0}} \\ &+ \sqrt{\frac{\lambda^2}{4\nu^2} \left(\frac{M_{\text{BH}}}{(M_h)_{\text{min},0}} \right)^2 + \frac{1}{4} \frac{a_*}{|a_s|}}. \end{aligned} \quad (\text{A2})$$

This expression coincides with the maximum core mass $(M_c)_{\text{max},*}$ given by Eq. (67) [see also Eqs. (23) and (66)].

-
- [1] Planck Collaboration, *Astron. Astrophys.* **571**, 66 (2014)
 - [2] Planck Collaboration, *Astron. Astrophys.* **594**, A13 (2016)
 - [3] J.F. Navarro, C.S. Frenk, S.D.M. White, *Astrophys. J.* **462**, 563 (1996)
 - [4] A. Burkert, *Astrophys. J.* **447**, L25 (1995)
 - [5] G. Kauffmann, S.D.M. White, B. Guiderdoni, *Mon. Not. R. astr. Soc.* **264**, 201 (1993); A. Klypin, A.V. Kravtsov, O. Valenzuela, *Astrophys. J.* **522**, 82 (1999); M. Kamionkowski, A.R. Liddle, *Phys. Rev. Lett.* **84**, 4525 (2000)
 - [6] M. Boylan-Kolchin, J.S. Bullock, M. Kaplinghat, *Mon. Not. R. Astron. Soc.* **415**, 40 (2011)
 - [7] P.H. Chavanis, *Phys. Rev. D* **84**, 043531 (2011)
 - [8] P.H. Chavanis, *Phys. Rev. D* **100**, 083022 (2019)
 - [9] A. Suárez, V.H. Robles, T. Matos, *Astrophys. Space Sci. Proc.* **38**, 107 (2014)
 - [10] T. Rindler-Daller, P.R. Shapiro, *Astrophys. Space Sci. Proc.* **38**, 163 (2014)
 - [11] P.H. Chavanis, *Self-gravitating Bose-Einstein condensates*, in *Quantum Aspects of Black Holes*, edited by X. Calmet (Springer, 2015)
 - [12] D. Marsh, *Phys. Rep.* **643**, 1 (2016)
 - [13] J.W. Lee, *EPJ Web of Conferences* **168**, 06005 (2018)
 - [14] E. Braaten, H. Zhang, arXiv:1810.11473
 - [15] A. Suárez, P.H. Chavanis, *Phys. Rev. D* **95**, 063515 (2017)
 - [16] P.H. Chavanis, arXiv:1905.08137 (to appear)
 - [17] B. Li, T. Rindler-Daller, P.R. Shapiro, *Phys. Rev. D* **89**, 083536 (2014)
 - [18] J. Fan, *Phys. Dark Univ.* **14**, 84 (2016)
 - [19] M. Reig, J.W.F. Valle, M. Yamada, arXiv:1905.01287
 - [20] D. Lynden-Bell, *Mon. Not. R. Astron. Soc.* **136**, 101 (1967)
 - [21] E. Seidel, W.M. Suen, *Phys. Rev. Lett.* **72**, 2516 (1994)
 - [22] F.S. Guzmán, L.A. Ureña-López, *Phys. Rev. D* **69**, 124033 (2004)
 - [23] F.S. Guzmán, L.A. Ureña-López, *Astrophys. J.* **645**, 814 (2006)
 - [24] H.Y. Schive, T. Chiueh, T. Broadhurst, *Nature Physics* **10**, 496 (2014)
 - [25] H.Y. Schive *et al.*, *Phys. Rev. Lett.* **113**, 261302 (2014)
 - [26] P. Mocz *et al.*, *Mon. Not. R. Astron. Soc.* **471**, 4559 (2017)
 - [27] J. Veltmaat, J.C. Niemeyer, B. Schwabe, *Phys. Rev. D* **98**, 043509 (2018)
 - [28] P. Mocz *et al.*, *Phys. Rev. Lett.* **123**, 141301 (2019)
 - [29] P.H. Chavanis, L. Delfini, *Phys. Rev. D* **84**, 043532 (2011)
 - [30] L. Hui, J. Ostriker, S. Tremaine, E. Witten, *Phys. Rev. D* **95**, 043541 (2017)
 - [31] B. Bar-Or, J.B. Fouvry, S. Tremaine, *Astrophys. J.* **871**, 28 (2019)
 - [32] P. Mocz, L. Lancaster, A. Fialkov, F. Becerra, P.H. Chavanis, *Phys. Rev. D* **97**, 083519 (2018)
 - [33] J. Binney, S. Tremaine, *Galactic Dynamics* (Princeton, NJ: Princeton University Press, 1987)
 - [34] J. Kormendy, K.C. Freeman, in S.D. Ryder, D.J. Pisano, M.A. Walker, K.C. Freeman, eds., *Proc. IAU Symp. 220, Dark Matter in Galaxies*. Astron. Soc. Pac., San Francisco, p. 377 (2004)
 - [35] M. Spano, M. Marcelin, P. Amram, C. Carignan, B. Epinat, O. Hernandez, *Mon. Not. R. Astron. Soc.* **383**, 297 (2008)
 - [36] F. Donato *et al.*, *Mon. Not. R. Astron. Soc.* **397**, 1169 (2009)
 - [37] N. Bar, D. Blas, K. Blum, S. Sibiryakov, *Phys. Rev. D* **98**, 083027 (2018)
 - [38] T. Padmanabhan, *Phys. Rep.* **188**, 285 (1990)
 - [39] J. Katz, *Found. Phys.* **33**, 223 (2003)
 - [40] P.H. Chavanis, *Int. J. Mod. Phys. B* **20**, 3113 (2006)
 - [41] D. Lynden-Bell, R. Wood, *Mon. Not. R. Astron. Soc.* **138**, 495 (1968)
 - [42] S. Balberg, S.L. Shapiro, S. Inagaki, *Astrophys. J.* **568**, 475 (2002)
 - [43] P.H. Chavanis, *Eur. Phys. J. Plus* **134**, 352 (2019)
 - [44] E.Y. Davies, P. Mocz, arXiv:1908.04790
 - [45] A.A. Avilez, L.E. Padilla, T. Bernal, T. Matos, *Mon. Not. R. Astron. Soc.* **477**, 3257 (2018)
 - [46] J. Eby, M. Leembruggen, P. Suranyi, L.C.R. Wijeward-

- hana, JCAP **10**, 058 (2018)
- [47] N. Bar, K. Blum, T. Lacroix, P. Panci, JCAP **07**, 045 (2019)
- [48] P. Brax, J.A.R. Cembranos, P. Valageas, arXiv:1909.02614
- [49] V. Desjacques, A. Nusser, Mon. Not. R. Astron. Soc. **488**, 4497 (2019)
- [50] L. Ferrarese, Astrophys. J. **578**, 90 (2002)
- [51] K. Bandara, D. Crampton, L. Simard, Astrophys. J. **704**, 1135 (2009)
- [52] P.H. Chavanis, Phys. Rev. D **98**, 023009 (2018)
- [53] E. Braaten, A. Mohapatra, H. Zhang, Phys. Rev. Lett. **117**, 121801 (2016)
- [54] E. Cotner, Phys. Rev. D **94**, 063503 (2016)
- [55] P.H. Chavanis, Phys. Rev. D **94**, 083007 (2016)
- [56] J. Eby *et al.*, JHEP **12**, 066 (2016)
- [57] D.G. Levkov, A.G. Panin, I.I. Tkachev, Phys. Rev. Lett. **118**, 011301 (2017)
- [58] T. Helfer *et al.*, JCAP **03**, 055 (2017)
- [59] L. Visinelli, S. Baum, J. Redondo, K. Freese, F. Wilczek, Phys. Lett. B **777**, 64 (2018)
- [60] F. Michel, I.G. Moss, Phys. Lett. B **785**, 9 (2018)